

### Supporting information

#### **One-step synthesis of an acceptor-donor-acceptor small molecule based on indacenodithieno[3,2-*b*]thiophene and benzothiadiazole units for high-performance solution-processed organic field-effect transistors**

Guobing Zhang,<sup>\*a, b</sup> Ruikun Chen,<sup>a</sup> Mingxiang Sun,<sup>a</sup> Minkyu Kim,<sup>c</sup> Weiwei Wang,<sup>a</sup>  
Longzhen Qiu,<sup>\*a</sup> Kilwon Cho,<sup>c</sup> Yunsheng Ding<sup>\*,b</sup>

<sup>a</sup>Special Display and Imaging Technology Innovation Center of Anhui Province, National Engineering Laboratory of Special Display Technology, Academy of Opto-Electronic Technology, Hefei University of Technology, Hefei, 230009, P. R. China

<sup>b</sup>School of Chemistry and Chemical Engineering, Hefei University of Technology, Key Laboratory of Advance Functional Materials and Devices of Anhui Province, Hefei, 23009, P. R. China

<sup>c</sup>Department of Chemical Engineering, Pohang University of Science and Technology, Pohang, 37673, Korea

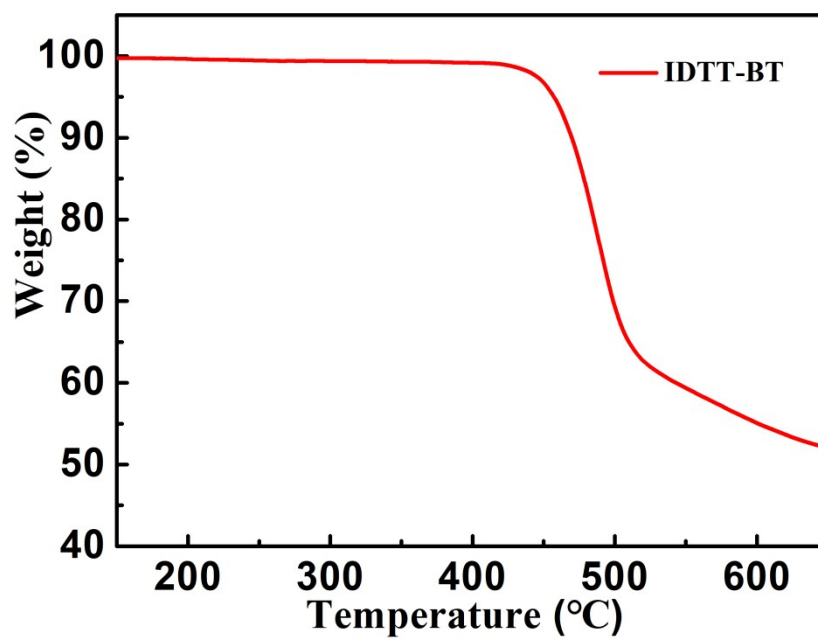


Fig. S1. The TG curve of IDTT-BT.

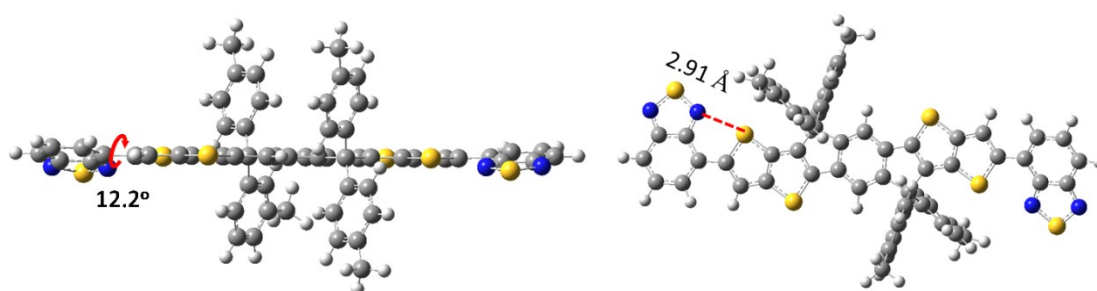
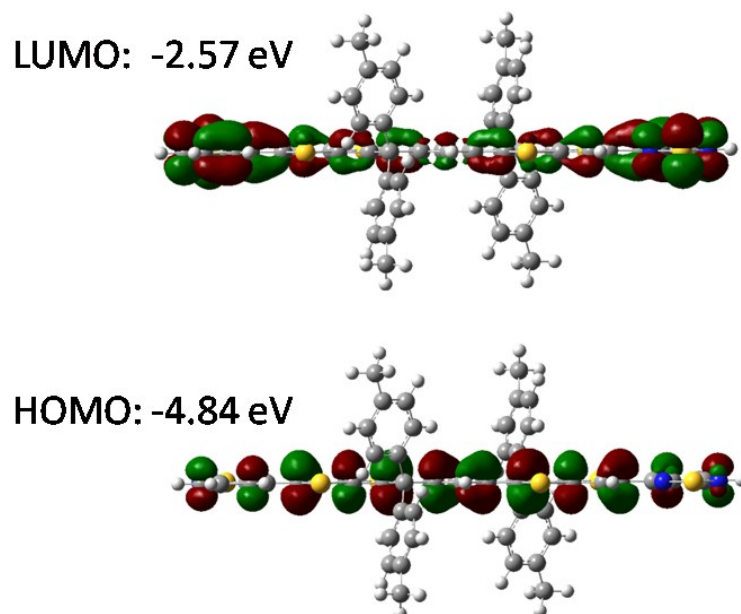


Fig. S2. DFT calculations of IDTT-BT based on S...N interactions using B3LYP/6-31G(d) level. The calculated S...N distance is 2.91 Å, much smaller than the calculated sum of Van der Waals radii of 3.20 Å.



**Fig. S3.** The calculated LUMO/HOMO energy levels according to DFT calculations at the B3LYP/6-31G(d) level.

**Table S1.** The device performances of **IDTT-BT**-based OFETs.

Molecule	Annealing temperature (°C)	$\mu_{h,max}$ (cm <sup>2</sup> V <sup>-1</sup> s <sup>-1</sup> )	$\mu_{h,avg}^a$ (cm <sup>2</sup> V <sup>-1</sup> s <sup>-1</sup> )	$V_{th}$ (V)	$I_{on}/I_{off}$	$r$
<b>IDTT-BT</b>	N/A	/	/	/	/	/
	150	1.15	1.08 ± 0.06	-3.0	4.9 × 10 <sup>6</sup>	0.75
	180	1.59	1.51 ± 0.05	-2.2	8.1 × 10 <sup>6</sup>	0.77
	210	2.01	1.75 ± 0.13	-3.9	9.3 × 10 <sup>6</sup>	0.85
	240	0.62	0.53 ± 0.07	-3.1	9.6 × 10 <sup>6</sup>	0.83

<sup>a</sup>The values were obtained from 9-10 devices.

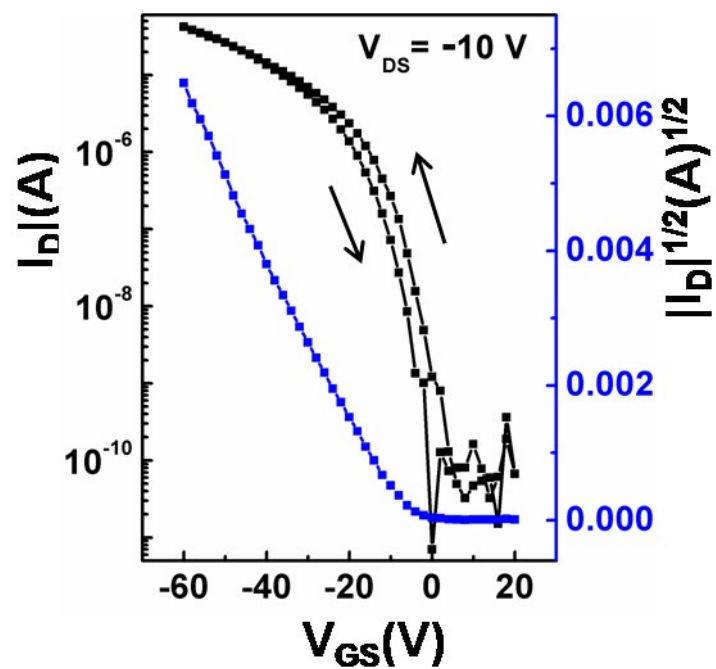


**Fig. S4.** The typical transfer curves of 210 °C-annealing devices characterized in low  $V_{ds}$  (-10 V).

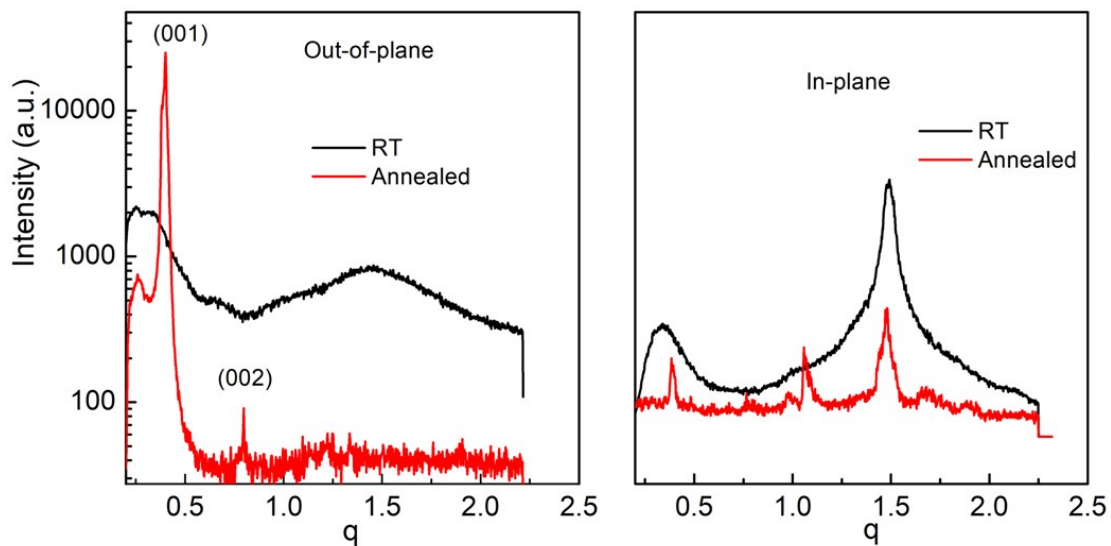


**Fig. S5.** Out-of-plane and in-plane line cuts of GIXD (RT and 210 °C).

## Experimental section

All the reagents were used as received without further purification. Tetrakis(4-hexylphenyl)-indacenodithieno[3,2-*b*]thiophene-bis-(trimethylstannane) and 4-bromo-2,1,3-benzothiadiazole were purchased from Derthon Optoelectronics Materials Science Technology Co. Ltd and Zhengzhou Alfa Chemical Co. Ltd, respectively. Tris(dibenzylideneacetone)dipalladium ( $\text{Pd}_2(\text{dba})_3$ ), tri(*o*-tolyl)phosphine ( $\text{P}(\text{o-tol})_3$ ), and other chemicals were purchased from Sigma-Aldrich Chemical Company, Alfa Aesar Chemical Company, and Sinopharm Chemical Reagent Co. Ltd., China.

### The synthesis of IDTT-BT

A Schlenk tube was charged with compound 4-bromo-2,1,3-benzothiadiazole (0.042 g, 0.20 mmol), tetrakis(4-hexylphenyl)-indacenodithieno[3,2-*b*]thiophene-bis(trimethylstannane) (0.11 g, 0.09 mmol), and chlorobenzene (10 mL). The solution was degassed by nitrogen flow for 40 min. Tri(dibenzylideneacetone)dipalladium ( $\text{Pd}_2(\text{dba})_3$ , 4 mg) and tri-*o*-tolylphosphine ( $\text{P}(\text{o-tolyl})_3$ , 5 mg) were added into the solution. The tube was capped and heated to 110 °C for 24 h. After cooling to room temperature, the mixture was poured into  $\text{H}_2\text{O}$  and extracted with chloroform. The combined organic layer was dried over anhydrous sodium sulfate. After removing the solvent, the residue was purified by silica gel column chromatography using a mixture of petroleum ether/dichloromethane (10:1) to afford a purple-red solid (80 mg, 76.2%).  $^1\text{H}$ NMR (400 MHz,  $\text{C}_2\text{Cl}_4\text{D}_2$ ):  $\delta$ = 8.61 (s, 2H), 7.90 (d, 2H), 7.80 (d, 2H), 7.62 (s, 2H), 7.59 (d, 2H), 7.26 (d, 8H), 7.17 (d, 8H), 2.59 (t, 8H), 1.60 (m, 8H), 1.30 (m, 24H), 0.87 (t, 12H).

$^{13}\text{C}$  NMR (400 MHz,  $\text{C}_2\text{Cl}_4\text{D}_2$ ):  $\delta$ = 154.94, 153.01, 151.23, 145.87, 143.74, 142.29, 141.31, 139.80, 139.35, 135.43, 133.46, 129.25, 128.06, 127.49, 127.00, 124.54, 121.63, 119.52, 116.67, 62.40, 35.05, 31.16, 30.71, 28.67, 22.10, 13.68.

Elemental Analysis: calcd for  $\text{C}_{80}\text{H}_{78}\text{N}_4\text{S}_6$  (%): C, 74.61, H, 6.10, N, 4.35, found (%) C, 74.95, H, 6.41, N, 4.12. MS (MALDI-TOF):  $m/z$  1286 ( $[\text{M}+\text{H}]^+$ ).

### Measurements and characterization

Nuclear magnetic resonance (NMR) spectra were recorded using an Agilent

VNMRS600 machine (400 MHz). Mass spectra were measured using GCT-MS EI and Bruker Daltonics Biflex MALDI-TOF Analyzer in the MALDI mode. Elemental analysis was performed by Vario MICRO. The single crystals were obtained by slow diffusion of methanol into chloroform solution at room temperature. The data were collected on a SuperNova, Dual, Cu at zero, AltasS2 diffractometer using graphite-monochromated Cu K $\alpha$  radiation ( $\lambda = 1.54 \text{ \AA}$ ). Thermogravimetric analysis (TGA) was conducted with a STA449F5 at a heating rate of 10 °C/min under nitrogen flow. UV-vis spectra were measured using solution in chloroform ( $1 \times 10^{-6} \text{ M}$ ) and films cast onto quartz glass using Agilent Cary 5000 model spectrophotometer. Electrochemical cyclic voltammetry (CV) was conducted under nitrogen using a CHI 660D electrochemical analyzer in anhydrous acetonitrile solution containing 0.1 M tetra-*n*-butylammounium hexafluorophosphate with a scan rate of 0.05 V/s. A platinum (Pt) electrode was used as both the working and auxiliary electrode. The Ag/Ag<sup>+</sup> electrode was used as the reference electrode. The AgNO<sub>3</sub> solution (0.1 M) was used in the characterization. HOMO =  $-(4.71 + E_{\text{onset}}^{\text{ox}})$  and LUMO =  $-(4.71 + E_{\text{onset}}^{\text{red}})$ ; the redox Fc/Fc<sup>+</sup> was located at 0.09 V related Ag/Ag<sup>+</sup>. Grazing-incidence-X-ray diffraction (GIXD) measurements were performed using 9A beamlines at the Pohang Accelerator Laboratory (PAL) in Korea. The fabrication of GIXD samples was same as the devices (In the Section of Device Fabrication). The atomic force microscopy (AFM) images were obtained using a SPA300HV instrument.

### **Fabrication and characterization of OFET device**

Bottom-gate/top-contact (BG/TC) OFETs devices were fabricated on a gate of *n*-doped Si with a 300-nm-thick SiO<sub>2</sub> dielectric layer (capacitance: 10.8 nF cm<sup>-2</sup>). The substrates were subjected to a piranha solution (70 vol% H<sub>2</sub>SO<sub>4</sub> and 30 vol% H<sub>2</sub>O<sub>2</sub>), followed by UV-ozone treatment. The surface of the wafer was modified with octadecyltrimethoxysilane (OTS) self-assembled monolayers (SAM) according to the previous procedures.<sup>[S1]</sup> Then, the IDTT-BT (5 mg) was added to the chloroform (1 mL), the mixture was stirred for about 3 h at 40 °C and the hot solution was dropped onto the OTS-treated Si/SiO<sub>2</sub> and spin-coated at 4000 rpm for 45 s in a glove box. The

small molecule films were annealed at different temperatures (150–240 °C, 30 min) in a glove box. The Au source-drain electrodes were prepared by thermal evaporation (~30 nm). The OFETs devices had a channel length ( $L$ ) of 130  $\mu\text{m}$  and a channel width ( $W$ ) of 760  $\mu\text{m}$ . The devices were characterized under air condition using a Keithley 4200 semiconductor parametric analyzer. The saturation-regime mobility ( $\mu$ ) was obtained using the following equation:  $I_d = (W/2L)C_i\mu_{sat}(V_g - V_{th})^2$ , where  $I_d$  is the drain current,  $C_i$  is the capacitance of the gate dielectric,  $V_g$  is the gate-source voltage,  $V_{th}$  is the threshold voltage, and  $V_d$  is the source-drain voltage.

The reliability factor ( $r$ ) was calculated by using the equation:<sup>[S2]</sup>

$$r = \left( \frac{\sqrt{|I_d|^{max}} - \sqrt{|I_d^0|}}{|V_g|^{max}} \right)^2 / \left( \frac{\partial \sqrt{|I_d|}}{\partial V_g} \right)^2$$

where  $|I_d|^{max}$  is the experimental maximum source-drain current reached at the maximum gate voltage  $|V_g|^{max}$ ,  $I_d^0$  is the source-drain current at  $V_G=0$ .

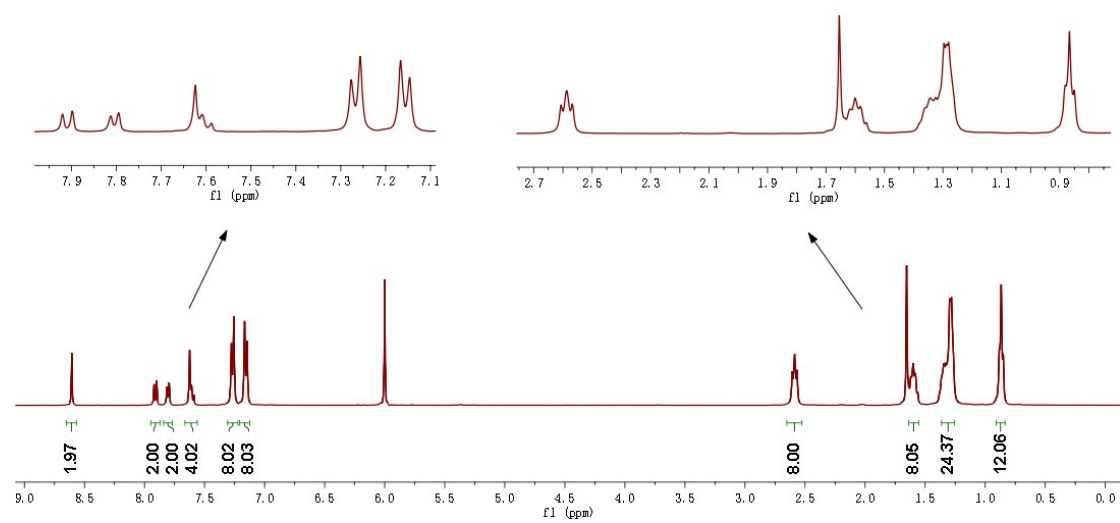


**Fig. S6.**  $^1\text{H}$  spectrum of IDTT-BT in  $\text{C}_2\text{Cl}_4\text{D}_2$ .

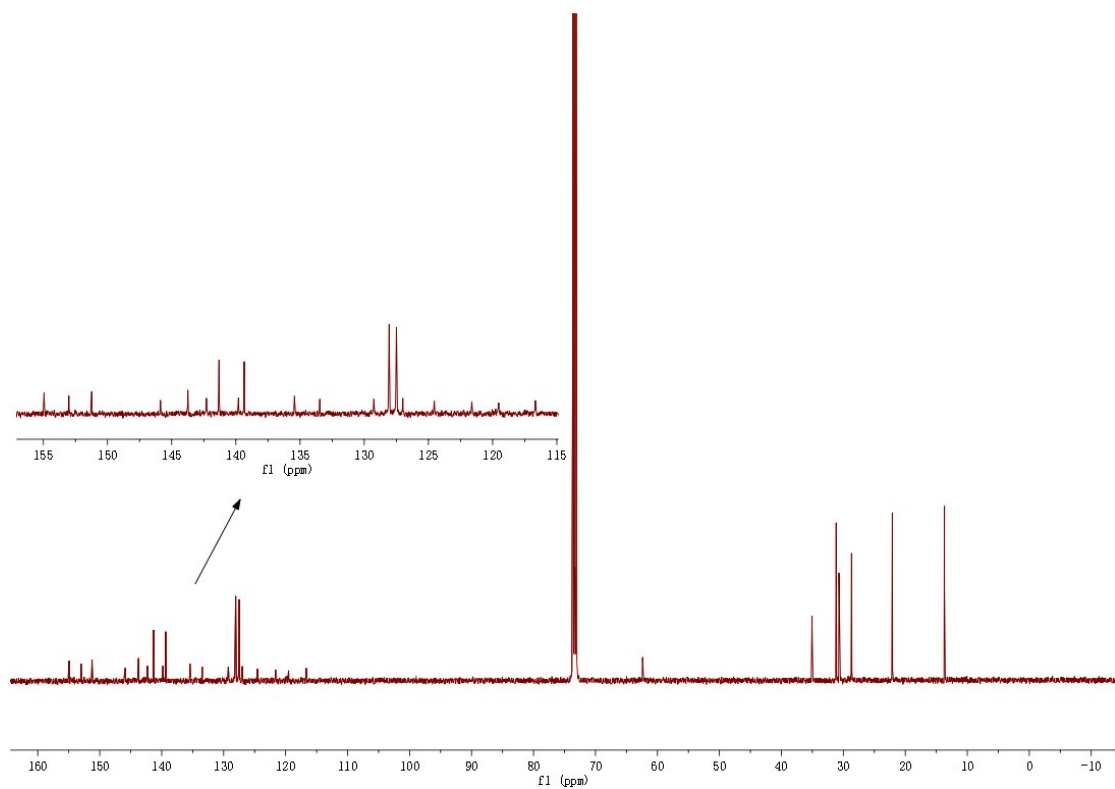


**Fig. S7.**  $^{13}\text{C}$  spectrum of IDTT-BT in  $\text{C}_2\text{Cl}_4\text{D}_2$ .

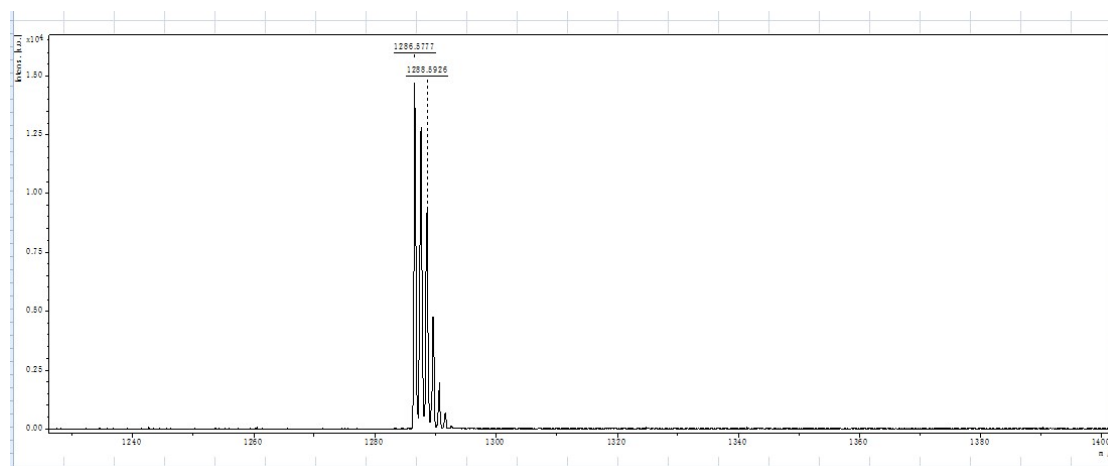


**Fig. S8.** The MALDI-TOF of **IDTT-BT**.

[S1] Ito, Y.; Virkar, A. A.; Mannsfeld, S.; Oh, J. H.; Toney, M.; Locklin, J.; Bao, Z. *J. Am. Chem. Soc.* **2009**, 131, 9396-9404.

[S2] Choi, H. H.; Cho, K.; Frisbie, C. D.; Sirringhaus, H.; Podzorov, V. *Nat. Mater.* **2018**, 17, 2-7.